Pub only

(5) 739200

(1)

$2.60

(5) 739200

(6) OPTIMUM TRAJECTORIES,

(10) by Arnold S. Mengel

P-199

January 15, 1951

The RAND Corporation
1700 MAIN ST. • SANTA MONICA • CALIFORNIA

28

P-199A
2-28-51

Abstract of Talk to be Given at Association for Computing Machinery Meeting at Wayne University, March 27-28, 1951.

Arnold S. Mengel

An analogue computer of the REAC type, although designed primarily for simulation, is a valuable tool in applied research. Several modifications have increased the flexibility and usefulness of the RAND REAC.

The REAC proved its worth in the study of the application of the calculus of variations to the optimization of aircraft flight paths. Prior to the installation of the REAC several reports on the theoretical aspects of the problem were written, but reached no conclusions because of the complexity of the equations. REAC solutions were of a surprising nature that not only led to unexpectedly practical answers, but also suggested revisions of the theory.

1-15-51
P-199

OPTIMUM TRAJECTORIES

Arnold S. Mengel

SUMMARY

The calculus of variations has been applied at RAND to answer such questions as

(1) What path should a missile with a fixed period of thrust fly to maximize its range at a specified final velocity and altitude?

(2) What path should an aircraft fly after take-off to minimize its time of flight to level-flight, combat velocity at a specified altitude?

The resulting equations are computationally difficult to handle because of their complexity and quasi-stable nature. Moreover, the new variables introduced by the calculus of variations have no apparent physical meaning, which makes the analysis of their influence difficult.

This paper outlines the experiences we have had at RAND solving calculus of variations problems on the REAC. A modified form of the equations (presented as an appendix to this paper) was developed which not only was more satisfactory computationally, but also showed that the calculus of variations equations described the motion of a body similar to the one under study. The nature of the REAC solutions suggested that the steady-state, or mid-path, trajectory and the transient trajectories from the steady-state path to the end-points could be computed separately. The results using this method agreed well with the "exact"* solution and gave a tremendous savings in computing time, since much of the trial-and-error process of meeting end-conditions in the usual process was eliminated and the stability problem was circumvented. Moreover, certain trajectories

*Quotation marks have been placed around the word exact, because certain approximations were necessary in the computation.

lent themselves to a simple servo-mechanism type analysis that gave results within 0.2 per cent of the "exact" optimum in one minute of MANIAC time compared to the eight hours required for the "exact" solution. However, certain missile equations were so complicated that the optimum paths had to be found by programming the flight paths and systematically searching for the maximums.

STATEMENT OF THE PROBLEM

Consider a body of weight w flying in two-dimensional space with a velocity v in a direction making an angle θ with the x-axis as shown in Figure 1. The total forces* acting on the body are resolved into four components, the weight vector $\vec{W}$, a force due to the change of weight $-\frac{\dot{w}}{g}\vec{V}$, a force vector $\vec{M}$ acting along the axis of the body, and a force $\vec{N}$ normal to its axis, with $\vec{F} = \vec{N} + \vec{M}$. The angle of attack α is the angle between the velocity vector $\vec{V}$ and the axis of the body. The magnitudes of $\vec{M}$ and $\vec{N}$ are assumed to be functions of the altitude y, velocity v, and angle of attack α. Defining $\vec{R}$ as the position vector of the body, with

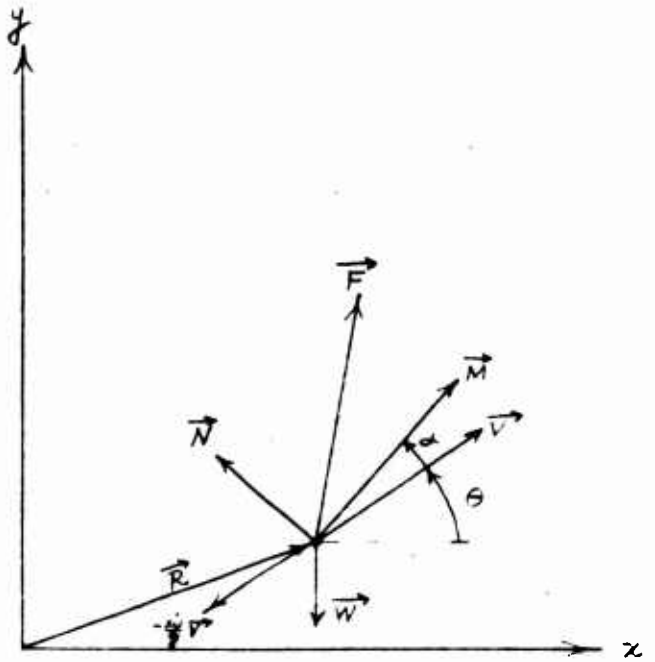

Figure 1. Forces on the Body

$$R = \sqrt{x^2 + y^2}$$

the dynamic equations are

*Neglecting the coriolis and centrifugal forces.

$$\left.\begin{aligned} \dot{\vec{R}} &= \vec{V} \\ \dot{\vec{V}} &= \frac{g}{w}\vec{F} + \vec{g} - \frac{\dot{w}}{w}\vec{V} \end{aligned}\right\} (1)$$

with initial conditions

$x = x_1$, $y = y_1$, $v = v_1$, $\theta = \theta_1$, $w = w_1$, and $t = t_1$.

The problem is to determine the path with terminal conditions

$x = x_2$, $y = y_2$, $v = v_2$, $\theta = \theta_2$, $w = w_2$, at $t = t_2$

such that one of the terminal variables is a minimum or maximum. The problem may be modified by not specifying certain terminal values, but if v_2 or θ_2 are not prescribed (or optimized) the problem becomes singular. The problem may be modified further by specifying constraints.

DISCUSSION

The problem posed in the previous section is not treated in the standard texts on the calculus of variations[1], and the first treatment of the problem at RAND was by E. M. Liebhold . Later, Dr. Magnus Hestenes, as a consultant, developed a more complete and elegant presentation [2,3]. The work of this paper was done with the cooperation of Dr. Hestenes, Kenneth Martin, and Roger Snow.

Application of the calculus of variations to the above problem yields a set of Euler-Lagrange differential equations (and variables) to be solved simultaneously with the dynamic equations of the system under study. The initial conditions of the Euler variables may be varied to cause the trajectory to pass through any possible set of end-conditions. Certain conditions must be satisfied to assure the solution is an optimum[2].

Unfortunately the Euler equations are usually considerably more complicated than the dynamic equations. Furthermore, the adjustment of the initial values of the Euler variables to meet specified end-conditions is a tedious trial-and-error process made more difficult by the absence of any physical significance for these variables. To make matters worse, the equations turn out to have a quasi-stable nature very similar to that of a neophyte tight-rope walker. This combination of woes led to the development of the equations appearing in the appendix.

The remainder of this paper will be a blow-by-blow description of our trials and tribulations with the calculus of variations. We hope to continue work on the problem at some future time.

Problem 1

Our first experience with a calculus of variations problem came when our acquaintanceship with the REAC was just starting and nearly resulted in a parting of the ways.

The purpose of this problem was to test how sensitive a maximum was to approximations made in the Euler equations. The body studied had constant weight, no lift, constant thrust, and drag proportional to the square of the velocity. The resulting dynamic and Euler equations were quite simple.

Our faces were crimson when the solutions of the approximate Euler Equations gave maximums several percent greater than those given by the exact equations. No manner of kicking, balancing, swearing, checking, and even cheating a bit on settings could deviate the REAC from its opinion that the approximate solution was the better.

Finally in desperation I derived the Euler equations and was overjoyed to find the problem had been submitted with a wrong sign in one of the Euler equations. Thus the REAC not only was vindicated, but at the same time was made a hero.

The corrected equations demonstrated, as hoped, that the optimums are flat enough that approximate trajectories give results for all practical purposes as good as the optimum trajectories.

Problem 2

This problem was a sequal to the above - an attempt to get a "feel" for trajectory optimization and to find the influence of the initial values of the Euler variables. A plot was made of final velocity v_2 as a function of final range x_2 for the body of Problem 1 at specified final values of altitude y_2, and time t_2 with zero final vertical velocity ($\theta_2 = 0$ or 180°).

It was hoped that a linearized set of equations would help in establishing the relationships between the initial values of the Euler variables to give the proper end-conditions, but since the partials changed rapidly and the inaccuracies introduced by taking differences were large, a plot of two of the variables versus the arctan of the third proved more helpful and at the same time gave some insight as to their influence on the system. The form of the plot of $\dot{x}_2$ versus x_2 is illustrated in Figure 2. Point A is the terminal pair for maximum $\dot{x}_2$ with x_2 not specified, while Point B is the terminal pair for maximum x_2 with $\dot{x}_2$ not specified. Actually, only the arc length designated AB is of any practical interest. It is apparent that since the lower portion of the

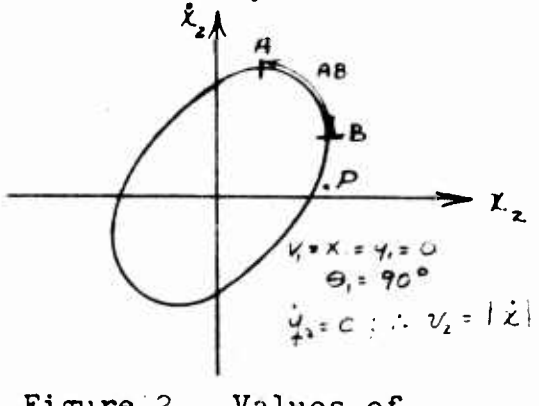

Figure 2. Values of $\dot{x}_2$ versus x_2 for specified y_2, θ_2, and t_2.

curve gives minimum values of $\dot{x}_2$ while the upper portion gives the maximum values, all other possible terminal conditions lie within the closed curve. For example, the system can not have a terminal condition such as specified by Point P.

Problem 3

To maximize the range of a missile it is necessary to study the power-on and power-off (or glide) stages separately. This problem was the power-on trajectory optimization. A set of values similar to the arc AB of Figure 2 was desired for several values of θ_2 and y_2 and was to be used as the initial values of the power-off trajectories.

The Euler equations for the power-on trajectory were too complicated to fit on our REAC and a trial-and-error process was required to give pseudo-optimum paths. Since the peaks appeared very flat and no better hand-controlled paths could be found, use of the resulting trajectories seemed justified.

The flight path was first programmed by letting $\dot{\theta} = a + \frac{b}{2}t$. The value of a was varied, b and θ_1 adjusted to meet the end-conditions and the sets found that gave maximums. The angle of attack giving the programmed $\dot{\theta}$ was computed and used in evaluating thrust and drag. A second method of programming with

$$\dot{\theta} = 0 \text{ for } 0 \leq t \leq \tau$$

$$\dot{\theta} = a + \frac{b}{2}(t - \tau) \text{ for } \tau \leq t \leq t_2$$

gave nearly identical maximums with what appeared at the time as more realistic trajectories.

Problem 4

During the power-off portion of the trajectory the velocity remained well above the speed of sound, the coefficients of lift and drag were reasonably well behaved and, as a consequence, it was possible to compute the dynamic plus Euler equations on the REAC. Since it was desired to maximize range with no regard to time, letting range be the independent variable and eliminating time greatly simplified the computation.

The trajectories were very sensitive to changes in the initial conditions of the two Euler variables and many trial runs had to be made to locate the region of interest. A typical set of trajectories with the initial value of one of the Euler variables fixed and the other varied is shown in Figure 3. A change of the initial value by about 5 per cent would swing the trajectory from path A to B. This great sensitivity and the quasi-stable condition is understandable when one considers the many end-conditions that must be possible no matter how undesirable they may be (i.e., vertical flight, reversed headings, etc.)

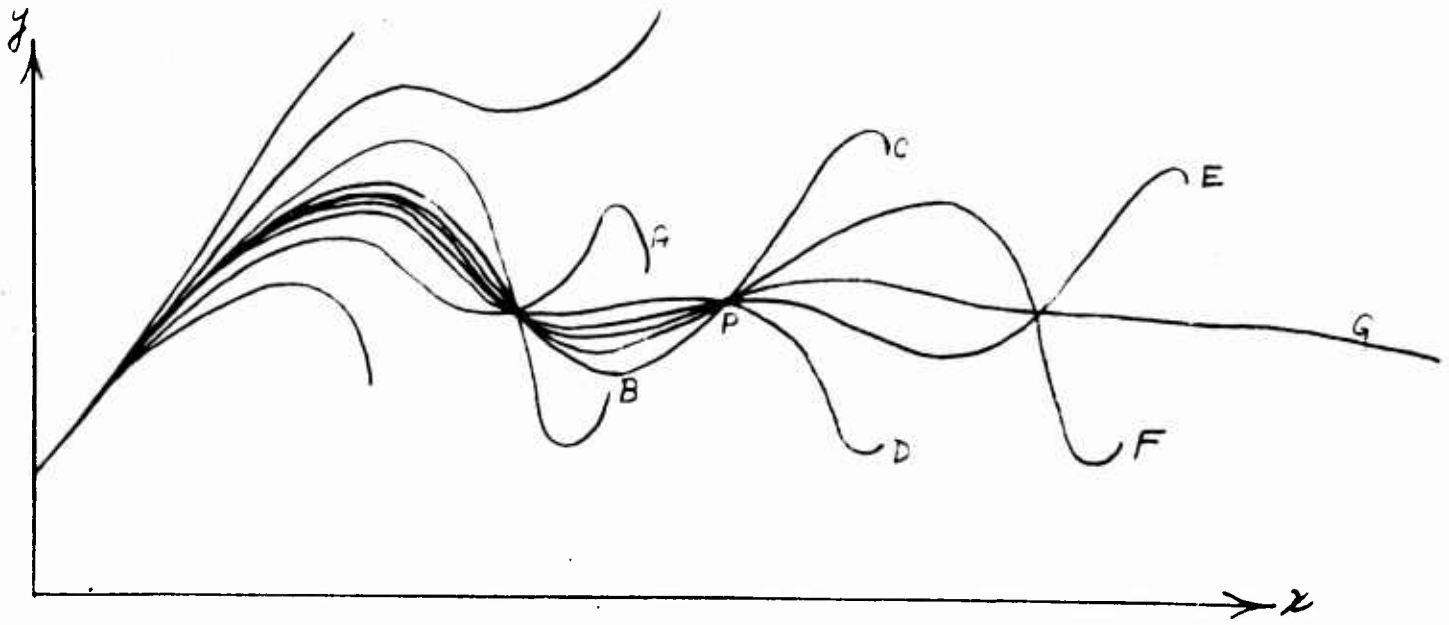

Figure 3. Typical Power-off Trajectories

It was apparent that the path giving maximum range was between A and B. Paths C and D were next found and differed by the order of about one per cent in the initial value of the Euler variable. The optimum path was between them; so using initial values between theirs we found the paths E and F, having the order of 0.1 per cent difference in their initial conditions. This discussion is based upon the assumption that the initial value held constant was at the proper value for the optimum path. Actually, the initial value of the second Euler variable would have to be "jockeyed" along with the other to keep the solutions from "blowing up". By the time path E and F were reached, the drift in the d.c. amplifiers prevented a continuation of the above procedure since the changes in the initial conditions became of the same order of magnitude as the drift. A simple change of scale-factor was impossible since the variables ranged from +100 to -100 volts despite their sensitivity to initial conditions.

An initial value bounded by those of paths E and F was selected, the problem stopped at the node P and readings made of the variables. These values, with perturbations on the Euler variables, were used as new initial conditions. This process was continued until the final velocity dropped to v_2 and required a full day of computing. Since this process had to be repeated for several sets of v_1, θ_1, and y_1, the prospects looked grim.

However, inspection of the first two days' results led to a much simpler computation. First it was noticed that the paths oscillated about the altitude for which lift equalled weight at the angle of attack α_c maximizing lift over drag. Moreover, the optimum paths approached this critical altitude in much the same way an underdamped servo-mechanism responds to a step function. Hence, we tried programming α as

$$\alpha = \alpha_c(1 - K \sin \theta)$$

where α_c was a function of velocity and K was varied until a maximum range was obtained. The unstable appearing end-conditions could be obtained by changing the sign in front of K; by varying K and the time of reversal of sign any end-conditions could be realized by paths similar to A through F of Figure 3. The values of range obtained by this approximate method were within 0.2 per cent of those found by the "exact" solution, and required about one minute of REAC time compared to the eight hours required for the "exact" solution.

Problem 5

The Euler and dynamic equations for an aircraft flying below the speed of sound are simple enough to handle on our REAC. In this problem we attempted to minimize time of flight from take-off to level flight, combat velocity at a specified altitude.

The first attempt at solution showed that the equations were even less stable than those of Problem 4. In fact, the paths dove into the ground no matter how the Euler variables were adjusted.

At this time the work of the appendix was started and it became apparent that the constraint $y \geq 0$ must be added, since an initial diving path to pick-up velocity was optimum. Obtaining a solution even with the computationally improved equations of the exact form in the appendix was still more difficult than for those of Problem 4 and again we were forced to develop an approximate method.

Previous work indicated that if the initial and final values were sufficiently separated, the mid-paths of all trajectories were nearly the same except near the transitions to the boundary values. Hence, as shown in the appendix, a quasi-steady state

solution was found giving the optimum midpath for all cases. The complete set of equations was used only for the transition from the mid-path to the end-points. Also equations were found giving either the optimum velocity or rate of climb at which to fly as functions of altitude, and the computation of the steady-state trajectory became simple enough for hand solution.

The dynamic equations for the hypothetical aircraft studied were

$$\dot{x} = v \cos \theta \text{ ft/sec}$$

$$\dot{y} = v \sin \theta \text{ ft/sec}$$

$$\dot{v} = \left[16 - 1.36\times10^{-5} v^2 - 3.13\times10^{-3}(v\alpha)^2\right]\sigma - 32.2 \sin \theta \text{ ft/sec}^2$$

$$\dot{\theta} = 3.13\times10^{-3}\sigma v\alpha - \frac{32.2 \cos \theta}{v} \text{ radians/sec.}$$

where σ = relative air density $\approx e^{-ay}$.

Figure 4 shows the form of the quasi-steady state solution plus one initial set of conditions and several final conditions. If the final velocity is approximately ten per cent or more than the climbing velocity, a final dive (as in Path A) is found to give quite a saving in time over a path leveling off at the desired altitude and flying level until the specified velocity is reached. A final steep climb before leveling-off is proper when a velocity less than the critical climbing velocity is desired. The initial portion of the trajectory was found by flying level until an α was called for making $\dot{\theta} > 0$ at which time the constraint $\dot{\theta} \geq 0$ was removed, as shown in Figure 5. A more satisfactory method would involve coming off the steady-state path with the complete equations as in the final portion of the trajectories but with time running backwards [5].

Figure 6 and the equivalent nomogram of Figure 7 give not only the minimum time of flight for specified values of v_2, y_2, and θ_2, but also the maximum value of y_2 with v_2, t_2, and θ_2 specified and the maximum value of v_2 with t_2, y_2, and θ_2 specified.

The optimum velocity and rate of climb for the hypothetical aircraft to fly as functions of altitude are given in Figures 8 and 9 respectively.

Comparisons of other flight programs with the optimum are illustrated by Figures 10 and 11. The aircraft climbed at a velocity Δv greater than the optimum in the first case and at a constant velocity in the second case. In both cases when the climbing velocity was less than the specified final value, the aircraft leveled off at the specified altitude and flew level until the desired velocity was reached. For those few cases where the climbing velocity was greater than the final value, the aircraft pulled into a climb before leveling-off.

It is difficult to justify mathematically the use of the quasi-steady state path for the major portion of the flight path and the use of the exact Euler equations only for the transition from the steady state path to and from the end points. However, the fact that the exact solutions follow the steady state path smoothly for a while and then oscillate about the steady state path when they "blow-up" is some justification. If then all optimum paths have very nearly identical midpaths, it becomes clear why the quasi-stable nature of the equations is necessary to make it possible to meet all end-points.

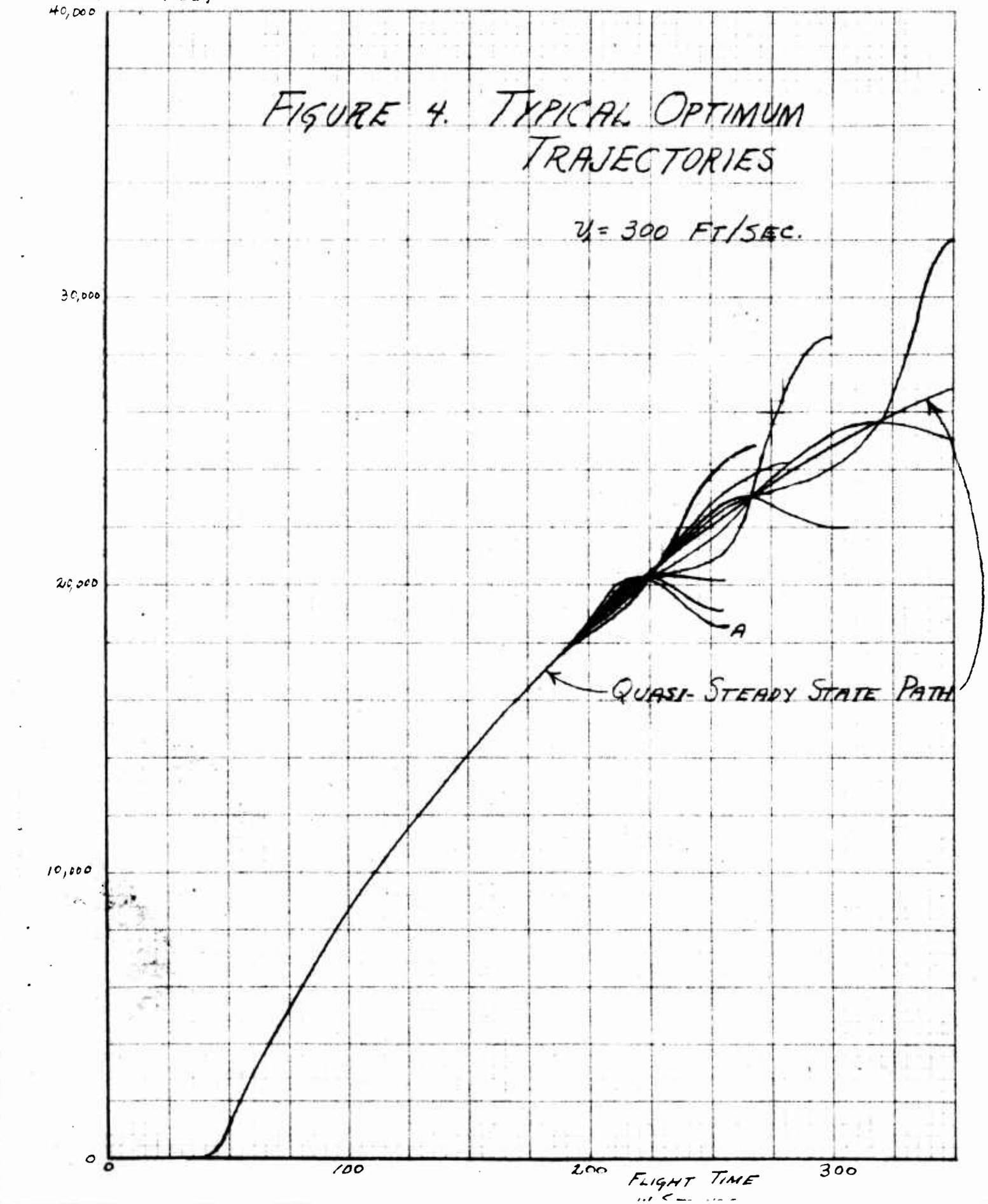

FIGURE 4. TYPICAL OPTIMUM TRAJECTORIES

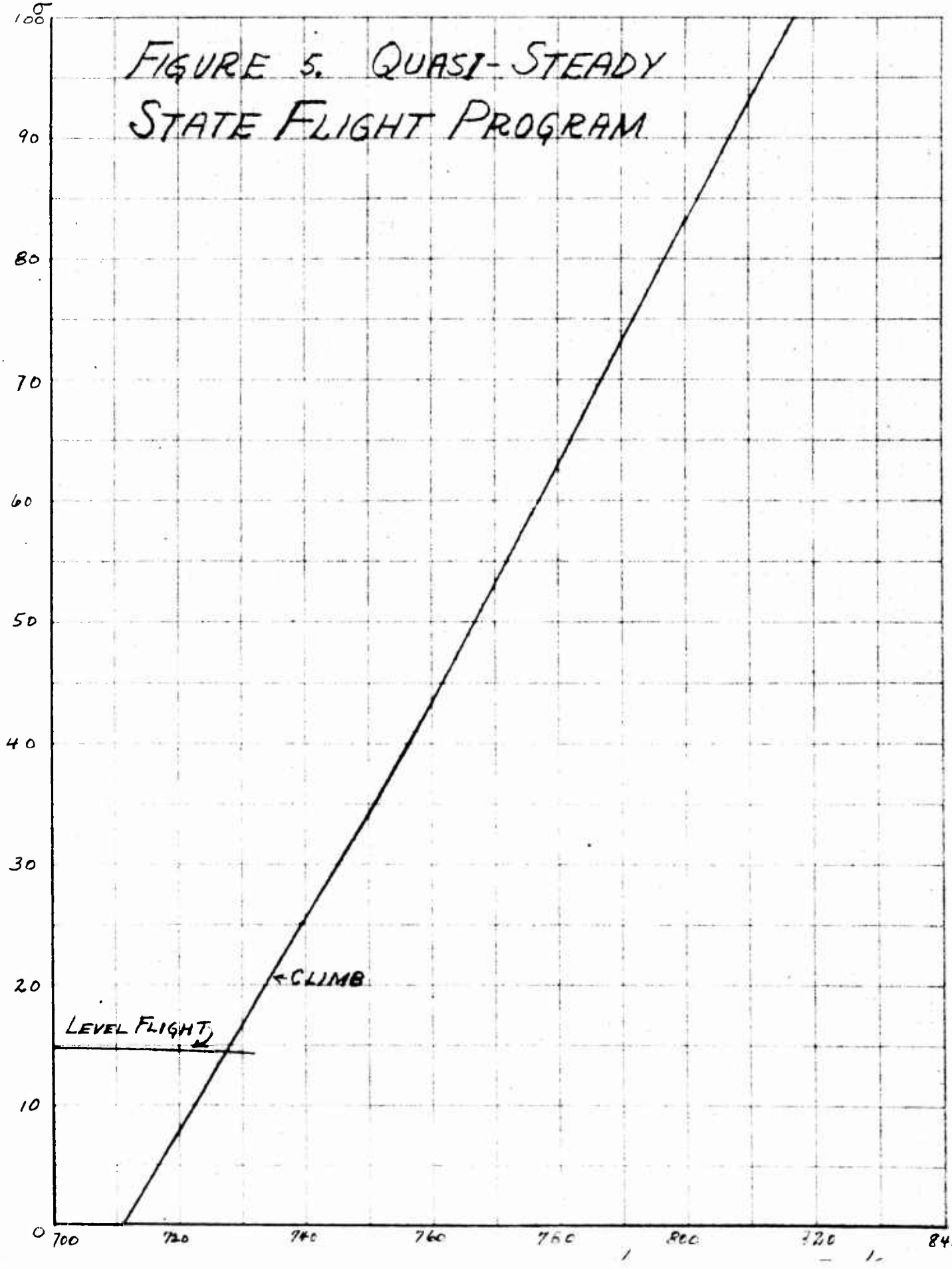

FIGURE 5. QUASI-STEADY STATE FLIGHT PROGRAM

FINAL ALTITUDE IN FEET

FIGURE 6. MINIMUM FLIGHT TIME VS. FINAL ALTITUDE AND VELOCITY

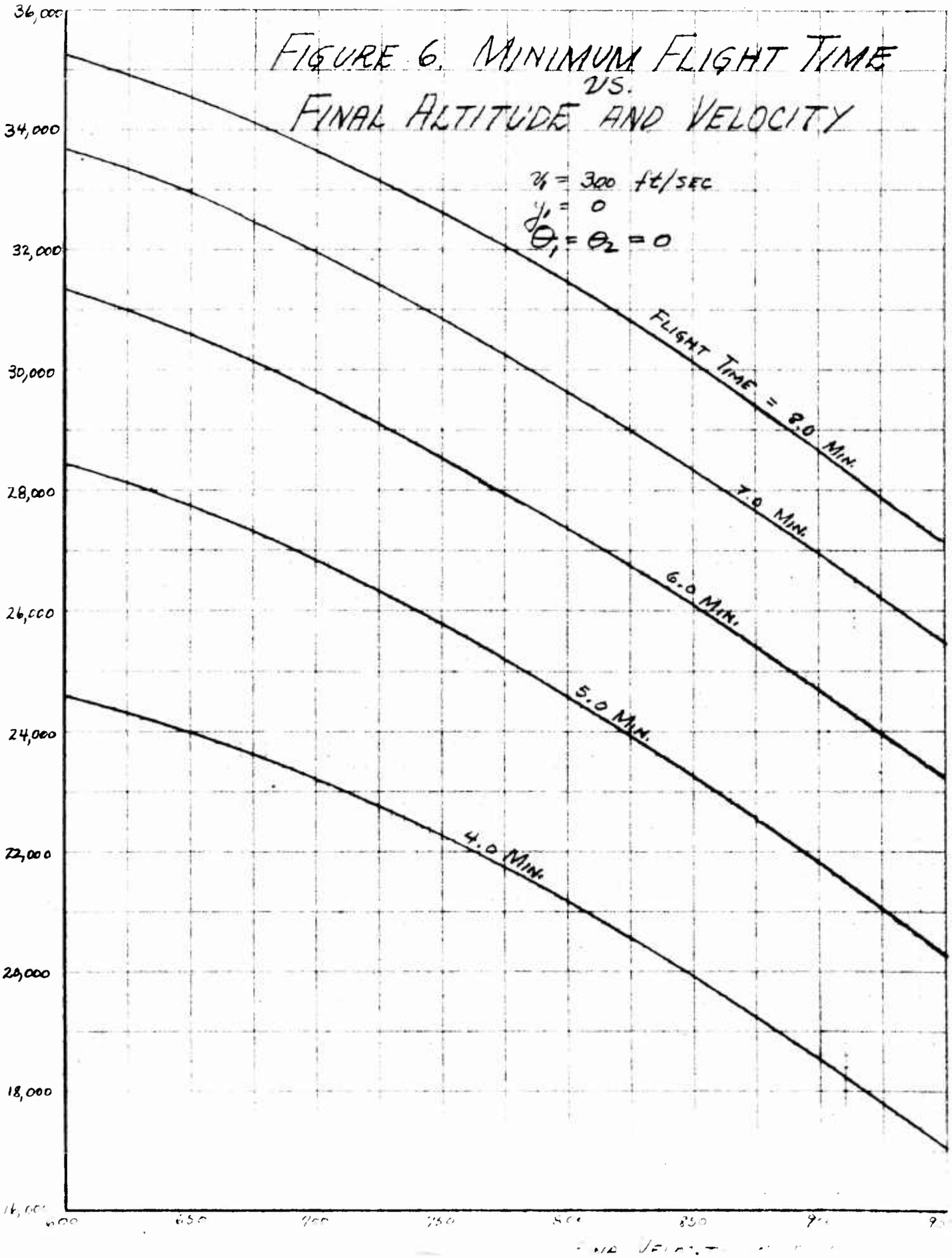

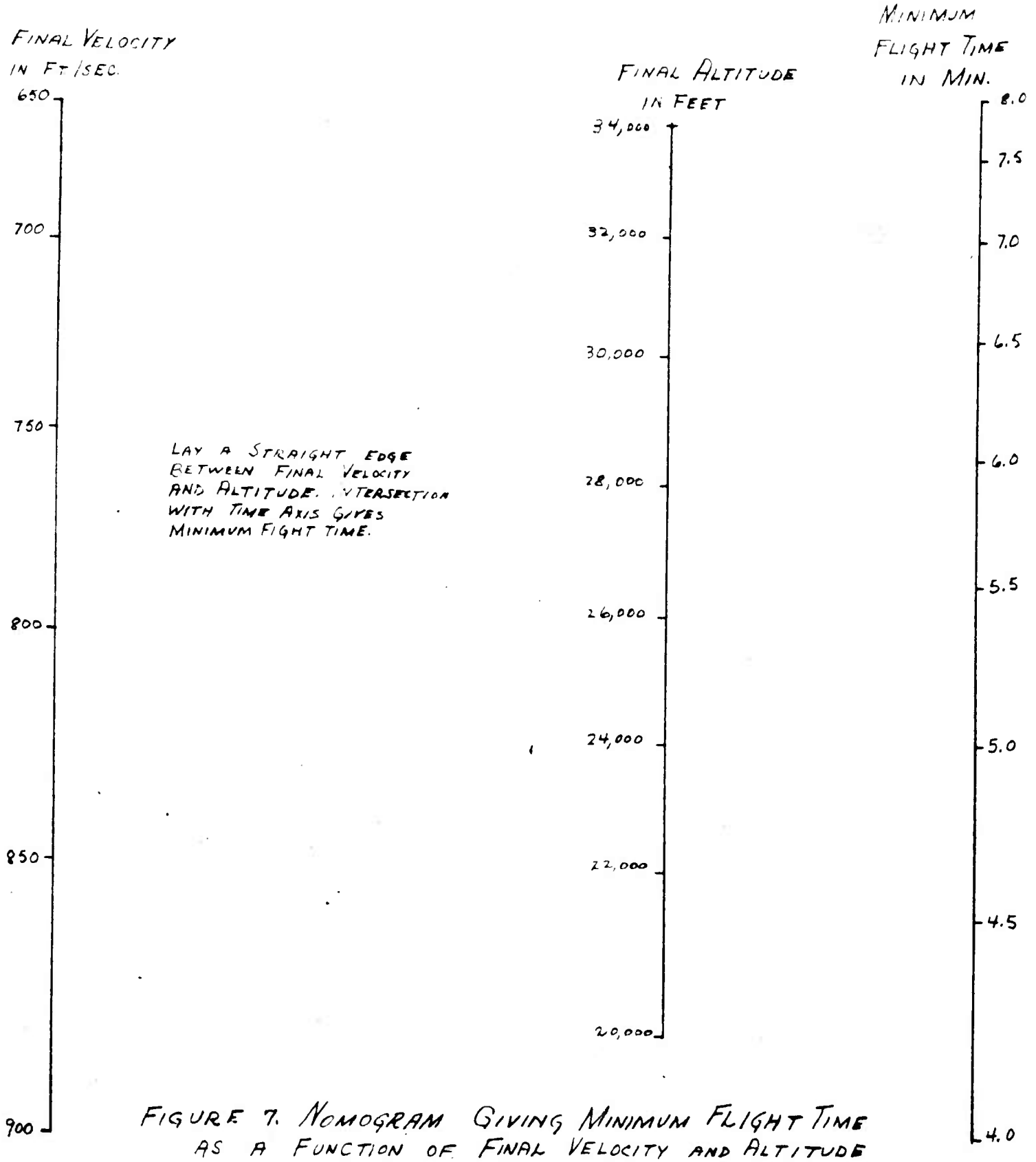

FIGURE 7. NOMOGRAM GIVING MINIMUM FLIGHT TIME AS A FUNCTION OF FINAL VELOCITY AND ALTITUDE

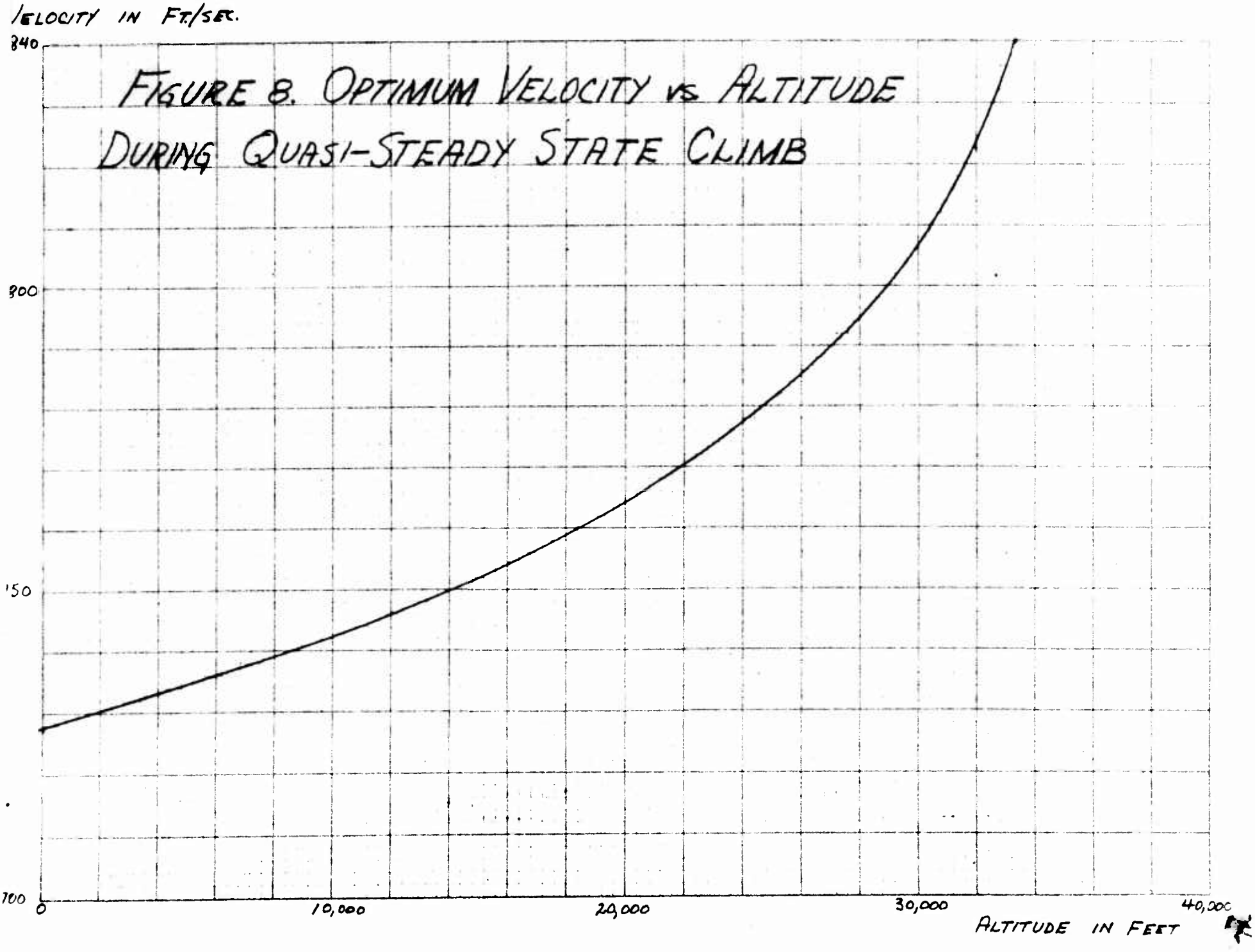

FIGURE 8. OPTIMUM VELOCITY VS ALTITUDE DURING QUASI-STEADY STATE CLIMB

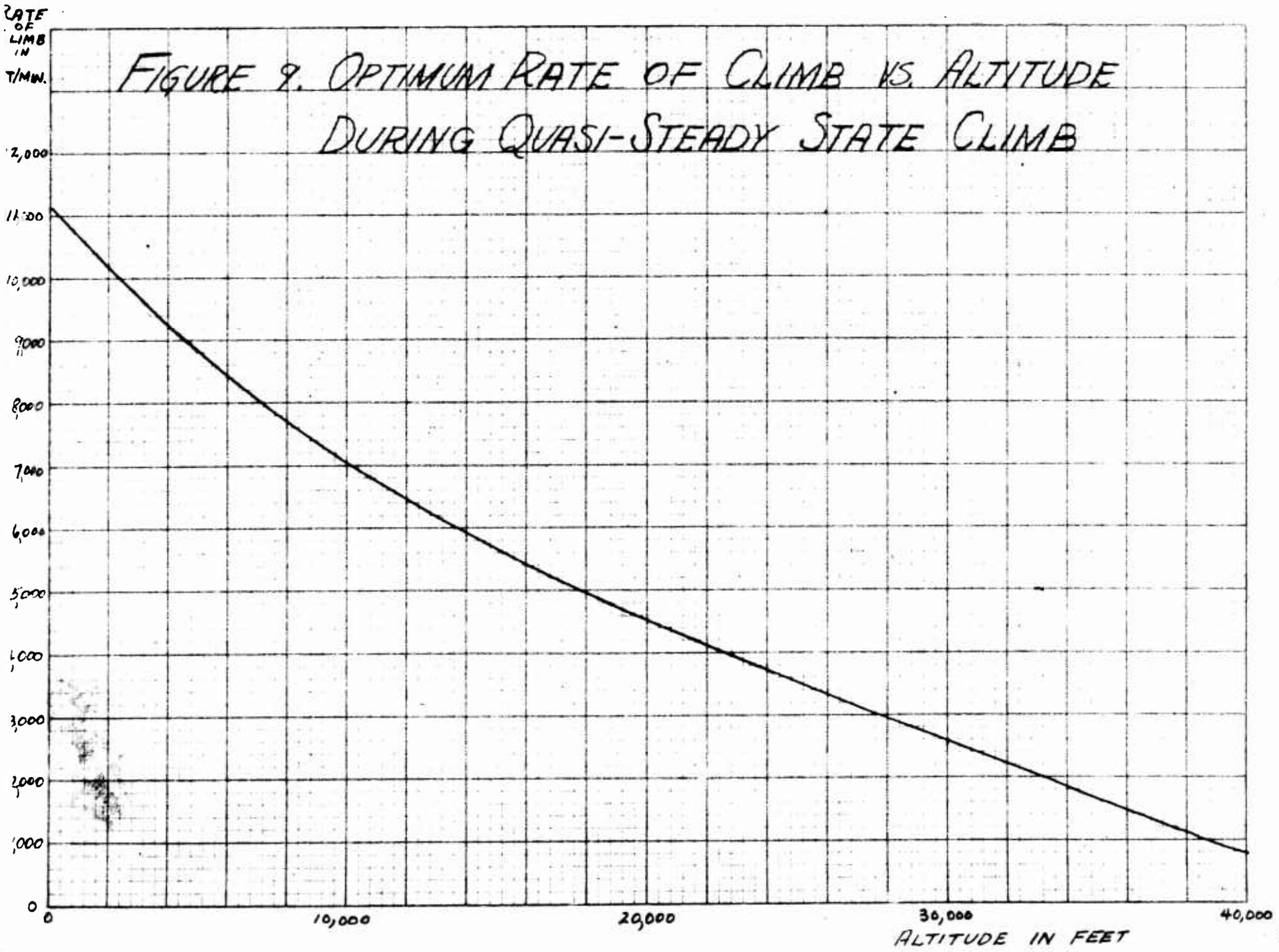

FIGURE 8. OPTIMUM RATE OF CLIMB VS. ALTITUDE DURING QUASI-STEADY STATE CLIMB

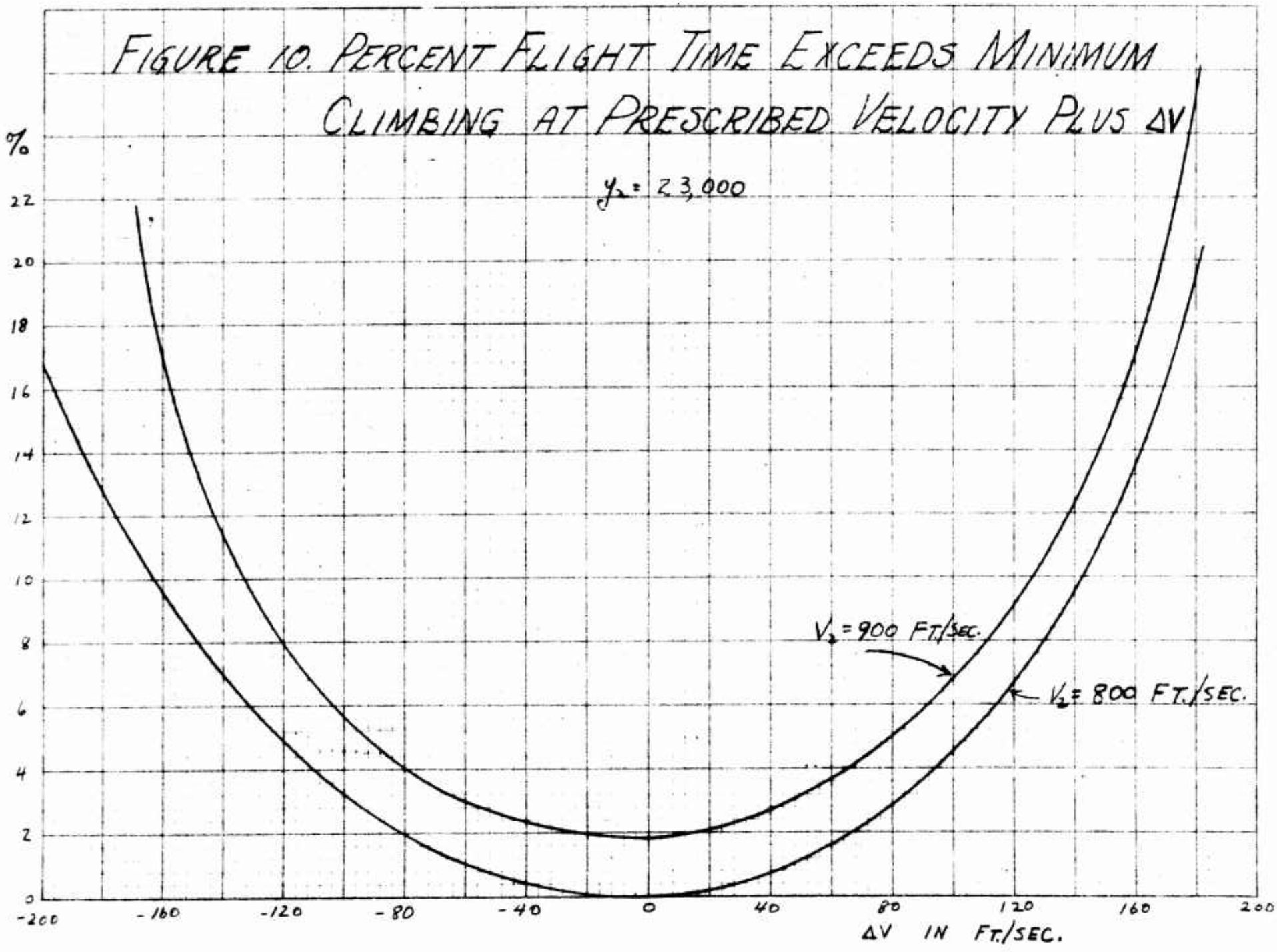
FIGURE 10. PERCENT FLIGHT TIME EXCEEDS MINIMUM CLIMBING AT PRESCRIBED VELOCITY PLUS ΔV
%
y_2 = 23,000
22
20
18
16
14
12
10
8
6
4
2
0
V_2 = 900 FT./SEC.
V_2 = 800 FT./SEC.
-200
-160
-120
-80
-40
0
40
80
120
160
200
ΔV IN FT./SEC.

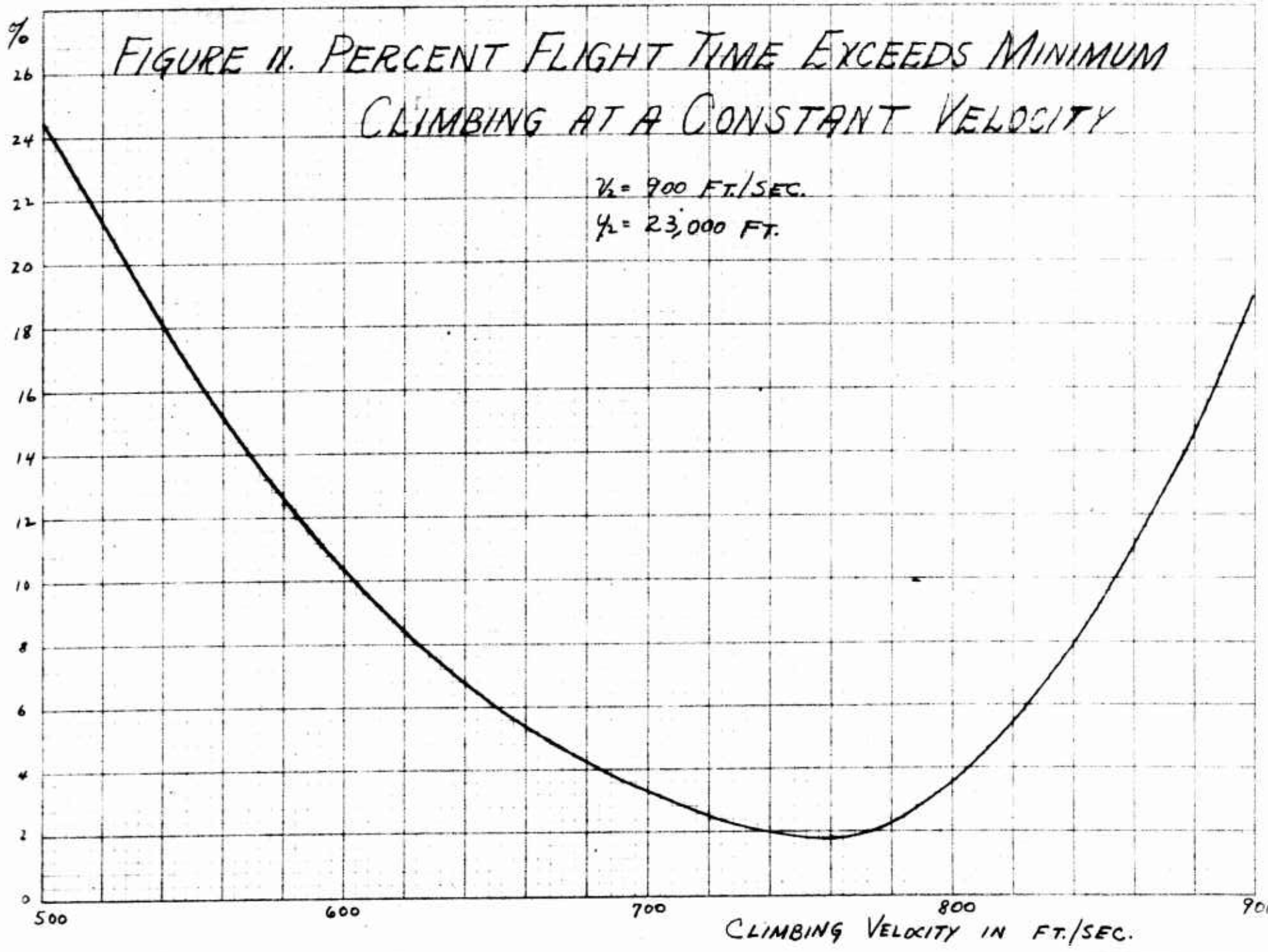

FIGURE 11. PERCENT FLIGHT TIME EXCEEDS MINIMUM CLIMBING AT A CONSTANT VELOCITY

V_2 = 900 FT./SEC.

Y_2 = 23,000 FT.

APPENDIX

BASIC EQUATIONS (assuming $\frac{\dot{W}}{W} \approx 0$)

Defining*

$$H = \vec{\lambda}\cdot\vec{V} + \vec{\mu}\cdot\dot{\vec{V}}$$

where $\vec{\lambda}$ and $\vec{\mu}$ are variable multipliers, the Euler-Lagrange equations optimizing the trajectory described by Figure 1 and Equations 1 are

$$\left.\begin{aligned} \dot{\vec{\lambda}} &= -\nabla_R H \\ \dot{\vec{\mu}} &= -\nabla_V H \\ H_\alpha &= 0 \end{aligned}\right\} \quad (2)$$

where

∇_R = gradient of H in $\vec{R}$ space

∇_V = gradient of H in $\vec{V}$ space

(the symbol ∇_R may be viewed as a partial gradient, i.e., the gradient when all variables but $\vec{R}$ are held fixed). Notice that the dynamic equations of motion are

$$\left.\begin{aligned} \dot{\vec{R}} &= \nabla_\lambda H \\ \dot{\vec{V}} &= \nabla_\mu H \end{aligned}\right\} \quad (1a)$$

Letting the argument of $\vec{\mu}$ be Φ, define

$$\left.\begin{aligned} \rho &= \Phi - \theta - \alpha \\ G &= M\cos\rho + N\sin\rho = \frac{\vec{\mu}}{\mu}\cdot\vec{F} \end{aligned}\right\} \quad (3)$$

or G is the projection of $\vec{F}$ on the vector $\vec{\mu}$. Then,

---

*The advantages of the vectorial derivation were pointed out by Roger Snow. This appendix assumes the reader is familiar with the theory of the calculus of variations given in RM-100.

$$\left.\begin{aligned} H &= \vec{\lambda}\cdot\vec{V} + \frac{g}{w}\mu G + \vec{\mu}\,\vec{g} \\ \dot{\vec{\lambda}} &= -\frac{g}{w}\mu\nabla_R G \\ \dot{\vec{\mu}} &= -\frac{g}{w}\mu\nabla_V G - \vec{\lambda} \\ H_\alpha &= \frac{g}{w}\mu\frac{\partial G}{\partial\alpha} = 0 \end{aligned}\right\} \quad (4)$$

Treating ρ as an independent variable

$$\left.\begin{aligned} G_V &= M_V \cos\rho + N_V \sin\rho \\ G_x &= 0 \\ G_y &= M_y \cos\rho + N_y \sin\rho \\ G_\alpha &= M_\alpha \cos\rho + N_\alpha \sin\rho \\ G_\rho &= -M \sin\rho + N \cos\rho \end{aligned}\right\} \quad (5)$$

Since $\rho = \phi - \theta - \alpha$

$$G_\theta = -G_\rho$$

$$\frac{\partial G}{\partial\alpha} = G_\alpha - G_\rho$$

and

$$H_\alpha = \mu(G_\alpha - G_\rho)\frac{g}{w} = 0$$

yields

$$G_\alpha = G_\rho$$

As a consequence, the last two equations of set 5 yield

$$M_\alpha \cos\rho + N_\alpha \sin\rho = -M \sin\rho + N \cos\rho$$

or

$$\rho = \arctan\frac{N - M_\alpha}{N_\alpha + M} \qquad (6)$$

Reducing the vector equations 1 and 4 to polar form gives

$$\left.\begin{aligned}
\dot{x} &= v\cos\theta \\
\dot{y} &= v\sin\theta \\
\dot{v} &= \frac{g}{w}(M\cos\alpha - N\sin\alpha) - g\sin\theta \\
v\dot{\theta} &= \frac{g}{w}(M\sin\alpha + N\cos\alpha) - g\cos\theta \\
\dot{\mu} &= \frac{g}{w}\left[-G_v\cos(\alpha+\rho) + \frac{G_\alpha}{v}\sin(\alpha+\rho)\right]\mu - \lambda_y\sin\phi - \lambda_x\cos\phi \\
\mu\dot{\phi} &= \frac{g}{w}\left[G_v\sin(\alpha+\rho) + \frac{G_\alpha}{v}\cos(\alpha+\rho)\right]\mu - \lambda_y\cos\phi + \lambda_x\sin\phi \\
\dot{\lambda}_x &= 0 \\
\dot{\lambda}_y &= -\frac{g}{w}G_y\mu \\
\rho &= \arctan\frac{N - M_\alpha}{N_\alpha + M}
\end{aligned}\right\} \quad (7)$$

in which G_θ has been replaced by the equivalent $-G_\alpha$.

It can be seen that the Euler equations describe a system acted upon by the forces shown in Figure 12. Thus these equations can be considered as describing the dynamics of an "Euler-craft" having an axial drag force μG_v, a normal lift force $\mu\frac{G_\alpha}{v}$, and two pseudo-gravity forces λ_y (variable) and λ_x (constant). The axis of the "Euler-craft" lies along the $\vec{V}$ vector and its "velocity" vector $\vec{\mu}$ is $(\alpha+\rho)$ radians above that of its axis.

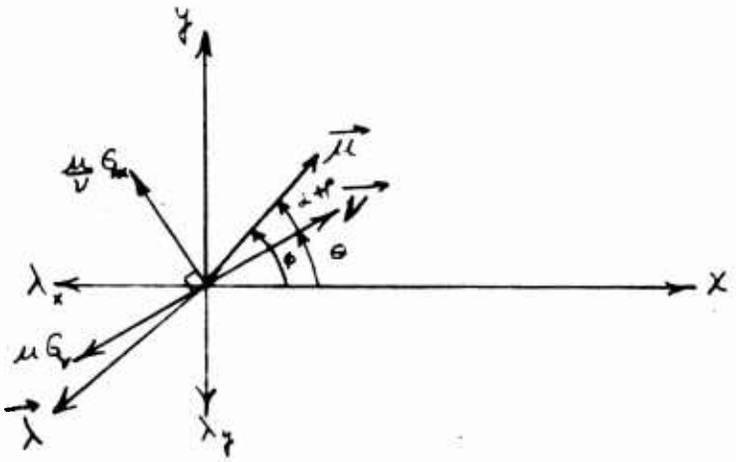

Figure 12. Forces on the "Euler-craft"

APPROXIMATE EQUATIONS

In general the forces on an aircraft are given by

$$\left.\begin{aligned} \frac{g}{w} M &= T(y,v) - f_1(y,v)\sigma v^2 \\ \frac{g}{w} N &= f_2(y,v)\sigma v^2 \alpha \end{aligned}\right\} \quad (8)$$

where

$\sigma \approx e^{-ay}$ is the relative air density and f_1 and f_2 are nearly constant for velocities below the speed of sound. As a consequence

$$\rho = \arctan \frac{N - M_\alpha}{N_\alpha + M} = \arctan \frac{f_2 \sigma v^2 \alpha}{T - f_1 \sigma v^2 + f_2 \sigma v^2} \approx \arctan \alpha \approx \alpha$$

since $T - f_1 \sigma v^2 \ll f_2 \sigma v^2$ and α is small.

If we neglect the influence of the axial forces on the equations for $\dot{\theta}$ and $\dot{\phi}$, and let $\rho = \alpha$, $\sin \alpha = \alpha$, $\sin 2\alpha = 2\alpha$, $\cos \alpha = 1$, and $\cos 2\alpha = 1$, equations 7 become

$$\left.\begin{aligned} \dot{x} &= v \cos \theta \\ \dot{y} &= v \sin \theta \\ \dot{v} &= \frac{g}{w}(M - N\alpha) - g \sin \theta \\ \dot{\theta} &= \frac{g}{w}\frac{N}{v} - \frac{g \cos \theta}{v} \\ \frac{\dot{\mu}}{\mu} &= \frac{g}{w}\left[-(M_v + \alpha N_v) + (M_\alpha + \alpha N_\alpha)2\alpha\right] - \frac{\lambda_y}{\mu} \sin \phi - \frac{\lambda_x}{\mu} \cos \phi \\ \dot{\phi} &= \frac{g}{w}\left[M_\alpha + \alpha N_\alpha\right] - \frac{\lambda_y}{\mu} \cos \phi + \frac{\lambda_x}{\mu} \sin \phi \\ \dot{\lambda}_x &= 0 \\ \frac{\dot{\lambda}_y}{\mu} &= -\frac{g}{w}\left[M_y + \alpha N_y\right] \end{aligned}\right\} \quad (9)$$

Since $\dot{\varphi} = (\theta + 2\alpha)$, $\alpha N_\alpha = N$, $vN_v \approx 2N$($f_1 \approx$ constant), and $M_\alpha = 0$, the Euler equations can be modified to

$$\left.\begin{aligned} 2\dot{\alpha} &= \frac{g}{v}\cos\theta - \frac{\lambda_y}{\mu}\cos(\theta + 2\alpha) + \frac{\lambda_x}{\mu}\sin(\theta + 2\alpha) \\ \frac{\dot{\mu}}{\mu} &= -\frac{g}{w}M_v - \frac{\lambda_y}{\mu}\sin(\theta + 2\alpha) - \frac{\lambda_x}{\mu}\cos(\theta + 2\alpha) \\ \frac{\dot{\lambda}_y}{\mu} &= -\frac{g}{w}\left[M_y + \alpha N_y\right] \end{aligned}\right\} \quad (10)$$

If the final range is not specified, $\lambda_x \equiv 0$, $\xi = \frac{\lambda_y}{\mu}$ is a convenient change of variable, and the Euler equations become

$$\left.\begin{aligned} 2\dot{\alpha} &= \frac{g\cos\theta}{v} - \xi\cos(\theta + 2\alpha) \\ \dot{\xi} &= -\frac{g}{w}\left[M_y + \alpha N_y\right] + \xi\left[\xi\sin(\theta + 2\alpha) + \frac{g}{w}M_v\right] \end{aligned}\right\} \quad (11)$$

Notice that once v_1, θ_1, and α_1 are set, the setting of ξ_1 determines $\dot{\alpha}_1$, thus clarifying the influence of the Euler variables.

QUASI-STEADY STATE CONDITIONS

During the quasi-steady state condition, $\dot{v}$, $\dot{\theta}$, α, $\dot{\alpha}$, and $\dot{\xi}$ will be small and we can use the approximations

$$\left.\begin{aligned} g\cos\theta &\approx \frac{g}{w}N \\ g\sin\theta &\approx \frac{g}{w}(M - N_\alpha) \\ \xi &\approx \frac{g}{v} \\ \frac{g}{w}\left[M_y + \alpha N_y\right] &\approx \frac{g}{v}\left[\frac{g}{v}\sin(\theta + 2\alpha) + \frac{g}{w}M_v\right] \end{aligned}\right\} \quad (12)$$

Since

$$g\sin(\theta + 2\alpha) \approx (g\cos\theta)2\alpha + g\sin\theta \approx \frac{g}{w}\left[M + N\alpha\right]$$

the last equation becomes $\left(\frac{v^2}{g}\frac{\partial}{\partial y} - \frac{\partial}{\partial v}\right)(M + \alpha N) = (N - \alpha M)$
or

$$v\left(\frac{v^2}{g}\frac{\partial}{\partial y} - \frac{\partial}{\partial v}\right) G = \vec{F}\cdot\vec{V} = \text{Rate of change of energy} \qquad (13)$$

This equation solved for α simultaneously with the dynamic equations yields the optimum quasi-steady state trajectory.

Putting equation 13 in the form of set 8 and assuming that the derivatives of the f functions with respect to y and v have only a second-order effect, we find

$$\frac{v^2}{g}\left(T_y + af_1\sigma v^2 - af_2\sigma(v\alpha)^2\right) - T + f_1\sigma v^2 - f_2\sigma(v\alpha)^2 \approx vT_v - 2f_1\sigma v^2$$

or

$$\alpha \approx \frac{\frac{v^2}{g}T_y - vT_v - T + \left(3 + a\frac{v^2}{g}\right)f_1\sigma v^2}{\varepsilon\left(1 + a\frac{v^2}{g}\right)\cos\theta} \qquad (14)$$

After take-off the plane should fly level (with $\dot{\theta} \geq 0$ constraint) until $\dot{\theta}$ becomes positive (at which time $\dot{\theta} \geq 0$ constraint is removed).

While this equation is suitable for REAC computation, in practice either the optimum velocity or optimum rate of climb as functions of altitude would be more useful to a pilot. Moreover, the $\left(\text{rate of climb}\right)^{-1}$ versus altitude curve can be integrated with respect to altitude to find the time of flight along the quasi-steady state path. The variable α can be eliminated by approximating it by that value it should have to keep $\dot{\theta} = 0$. To find the optimum velocity or rate of climb we must solve the simultaneous equations

$$\left.\begin{aligned} g^2\left(1 + a\frac{v^2}{g}\right)\cos^2\theta &\approx f_2\sigma v^2\left[\frac{v^2}{g}T_y - vT_v - T + \left(3 + a\frac{v^2}{g}\right)f_1\sigma v^2\right] \\ \sin\theta &\approx \frac{T - f_1\sigma v^2}{g} - \frac{g}{f_2\sigma v^2}\left[1 - \left(\frac{T - f_1\sigma v^2}{g}\right)^2\right]. \end{aligned}\right\} \qquad (15)$$

As a second approach, ξ and $\dot{\xi}$ may be eliminated by reducing the two first order differential equations of set 11 to one second order equation of the form

$$\ddot{\alpha} + F_1(y,v,\theta)\dot{\alpha} + F_2(y,v,\theta)\alpha = F_3(y,v,\theta). \qquad (16)$$

During the quasi-steady state portion of the flight path this equation reduces to

$$\alpha = \frac{F_3(y,v,\theta)}{F_2(y,v,\theta)} . \qquad (17)$$

As a third approach, we can use

$$\frac{g \cos \theta}{v} - \xi \cos (\theta + 2\alpha) = 0$$

to solve implicitly[8] for ξ,

$$-\frac{\xi}{w}\left[M_y + \alpha N_y\right] + \xi\left[\xi \sin (\theta + 2\alpha) + \frac{\xi}{w} N_v\right] = 0$$

to solve implicitly for α,

$$\frac{\xi}{w}(M - \alpha N) - g \sin \theta = 0$$

to solve implicitly for θ, and

$$\frac{\xi}{w} N - g \cos \theta = 0$$

to solve for implicitly for v. This method works particularly well on the REAC for it is possible to wire the problem such that one can switch from the steady-state solution to the transient solution during a run. It also is convenient to allow reversal of time to find initial as well as final transient paths.[5]

REFERENCES

1) G. A. Bliss, Lectures on the Calculus of Variations; University of Chicago Press, 1946.

2) M. R. Hestenes, A General Problem in the Calculus of Variations with Applications to Paths of Least Time; Project RAND Report RM-100, March 1, 1949.

3) M. R. Hestenes, Numerical Methods of Obtaining Solutions of Fixed End Point Problems in the Calculus of Variations; Project RAND Report RM-102, August 15, 1949.

4) A. S. Mengel, New Form of Euler Equations for Optimum Flight; Project RAND Report RM-307, January 6, 1950. This report is of little value because of numerous typographical errors.

5) A. S. Mengel and W. S. Melahn, RAND REAC Operators' Manual; Project RAND Report RM-525, December 1, 1950.